



Towards Targeted Antimalarial Therapies: A Review of Computational Methods in *PfDHODH* Inhibition

Thejus Varghese Thomas, Amrita Thakur* and S Anil Kumar

Abstract

Malaria continues to be a significant global health concern, with the risk of resurgence heightened by climate change and rising infection rates. In response, recent drug discovery efforts have identified *Plasmodium falciparum* dihydroorotate dehydrogenase (*PfDHODH*) as a promising antimalarial target. Computational approaches have been instrumental in accelerating the identification and optimization of *PfDHODH* inhibitors, providing innovative strategies for drug design. This review examines the growing role of computational techniques in the discovery of novel *PfDHODH* inhibitors, emphasizing key methodologies explored in recent years. The comprehensive review analyses published studies on the development of novel *PfDHODH* inhibitors, focusing on molecular scaffolds and optimization strategies aimed at enhancing drug efficacy. It highlights methodologies employed in novel compound development and synthesizes key findings from each study. Additionally, it discusses the contributions of molecular docking and molecular dynamics (MD) simulations in identifying crucial binding sites. By providing insights into essential molecular features for successful *PfDHODH* drug design and drug-inhibitor interactions, this review enhances the understanding of structural insights, binding mechanisms, and computational techniques utilized in the drug discovery process.

Keywords: Malaria, *PfDHODH* inhibitors, Computational drug design, Drug-inhibitor interactions, Pharmacophore modelling.
Received: 03 April 2025; Revised: 06 June 2025; Accepted: 21 July 2025
Article type: Review article.

1. Introduction

Malaria has significantly shaped human history, influencing migration, genetics, and colonization, particularly in Africa, Asia, and the Americas.^[1-6] It remains a critical health issue in impoverished regions, with climate change heightening resurgence risks.^[7-9] Annually, malaria affects over 200 million individuals, causing 500,000 deaths, predominantly due to *P. falciparum* and *P. vivax*.^[10-12] Antimalarial drugs have evolved to target the malaria parasite's lifecycle, which involves transitions between human hosts and mosquito vectors, beginning when female *Anopheles* mosquitoes inject sporozoites into the bloodstream. These sporozoites invade liver cells, where they mature into schizonts and release merozoites. The merozoites then infect red blood cells, consuming hemoglobin for nutrients and producing toxic heme as a by-product. To neutralize this toxicity, the parasite converts heme into non-toxic hemozoin crystals within the

acidic environment of the food vacuole. The merozoites replicate within red blood cells, releasing more merozoites that continue to infect additional red blood cells, perpetuating the cycle. Some merozoites differentiate into gametocytes, the sexual form of the parasite, which are ingested by mosquitoes during feeding, allowing the lifecycle to continue within the mosquito. This complex process highlights the parasite's adaptability and underscores the challenges in controlling malaria. Disrupting mechanisms such as hemoglobin metabolism and hemozoin formation presents opportunities for developing drugs to combat *Plasmodium falciparum*.^[13-16]

Fig. 1 summarizes the available therapies. Artemisinin-based Combination Therapies (ACTs) are the primary treatment for uncomplicated malaria, with chloroquine and Hydroxychloroquine (HCQ) for severe cases.^[17] WHO has also approved malaria vaccines RTS, S/AS01 and R21/Matrix-M show ~75% efficacy in children in seasonal malaria regions.^[18] In spite of available options, complete eradication is hindered by rising cases, African child mortality, and ACT-resistant *Plasmodium falciparum* strains with K13 mutations, necessitating new drug strategies.^[19]

The recent exploration of the *Plasmodium falciparum*

Department of Physical Sciences, Amrita School of Engineering, Amrita Vishwa Vidyapeetham, Bengaluru Campus, Bengaluru, Karnataka, 560035, India

*Email: t_amrita@blr.amrita.edu (A. Thakur)

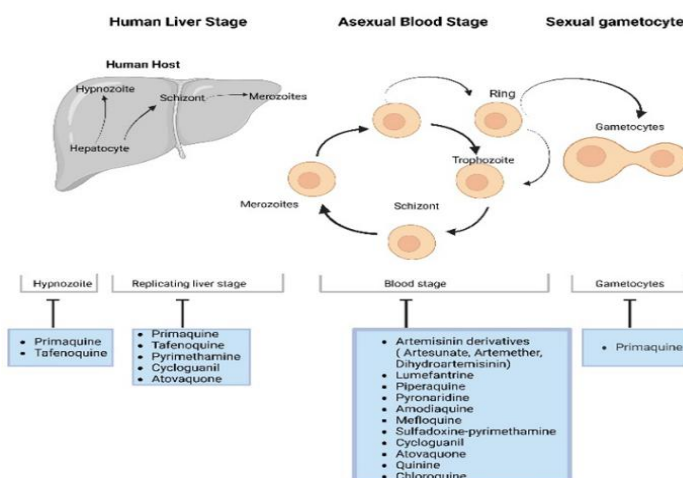


Fig. 1: The lifecycle of the plasmodium parasite and malaria therapeutics developed around it.

genome and deeper insights into parasite biology have accelerated the search for novel and effective antimalarial drugs. Promising candidates in various stages of development include DSM265,^[20] Genz-669178,^[21] and DSM421,^[22] targeting *PfDHODH* through collaborations with Medicines for Malaria Venture (MMV). Other proposed drug candidates like KAF156 disrupts protein synthesis, SJ733 affects sodium homeostasis,^[23] P218 inhibits DHFR,^[24] and OZ439, an artemisinin-like compound, showed initial promise but was discontinued in combination trials with DSM265 due to limited transmission-blocking efficacy and dosing challenges.^[25]

DSM265 is one of the most advanced *PfDHODH* inhibitors, showing effectiveness in human trials as a single-dose therapy. KAF156 (Ganaplacide)^[26] and OZ439 (Artefenomel)^[25] are notable as they have entered late-stage trials, with strong efficacy in both blood and liver stages of malaria. SJ733 and Genz-669178 are still in preclinical development, reflecting potential in *PfDHODH* inhibition.^[27]

Most of the antimalarials target key Plasmodium pathways, including heme detoxification, apicoplast function, electron transport, and DNA synthesis, with pyrimidines being crucial for nucleic acid biosynthesis within the parasite.^[28] *PfDHODH* has emerged as a crucial drug target due to its essential role in pyrimidine biosynthesis, selectivity over human DHODH, effectiveness against drug-resistant malaria, multi-stage activity, and potential for next-generation antimalarial development.

2. *PfDHODH*: A Promising drug target

Cells obtain pyrimidines through de novo synthesis, beginning by ammonia, aspartate, and bicarbonate, or by salvaging bases like uracil, cytosine, and thymine or nucleosides like uridine, thymidine, and cytidine. Notably, Plasmodium species rely exclusively on the de novo pathway due to their lack of enzymes for pyrimidine salvage. This pathway (Fig. 2) involves six key enzymes, among which *PfDHODH* stands out as a promising target.^[29]

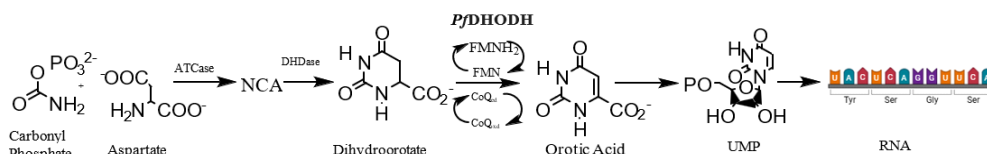


Fig. 2: Pyrimidine synthesis pathway.

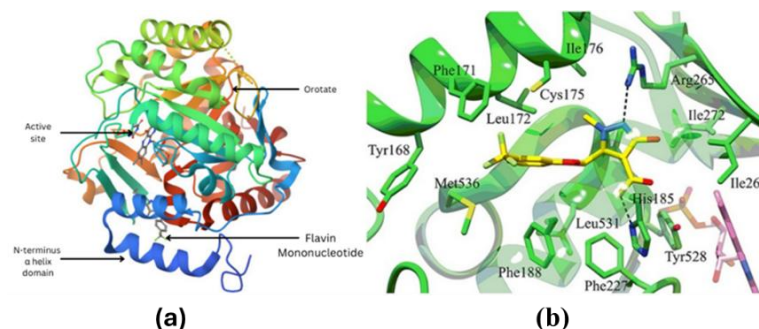


Fig. 3: a) PDB ID: 6VTY labelled with Canva web resource; b) Key Binding sites of *PfDHODH* with DSM265 (Copyright and permission acquired from Kokkonda *et al.* Reproduced from.^[35] - License No:5943421417850).

In de novo pyrimidine biosynthesis, DHODH oxidizes dihydroorotate to orotate via ubiquinone, thus providing an essential monomer for RNA synthesis. ATCase – Aspartate Transe Carbamoylase, DHOase – Dihydroorotase, NCA – Carbamoyl aspartate, UMP – Uridine Monophosphate, RNA – Ribonucleic acid.^[29] *Pf*DHODH, a 566-amino-acid enzyme catalyses the oxidation of dihydroorotate to orotate via a two-step process mediated by flavin mononucleotide (FMN) and coenzyme Q (CoQ). Its enzymatic activity relies on three critical structural features: the Catalytic Domain (β/α -barrel fold), spanning residues 162–565, which carries out the oxidation reaction,^[30] the N-terminal region anchors the enzyme to the mitochondrial inner membrane and positions the catalytic domain within the inner membrane space; the CoQ binding site is a flexible, hydrophobic pocket adjacent to FMN, facilitating strong binding to various small molecules, thereby serving as a significant drug target. This structural uniqueness of *Pf*DHODH, along with its essentiality for pyrimidine biosynthesis, makes it a validated drug target for antimalarial therapies. Notably, inhibitors targeting the CoQ site, such as triazolopyrimidine derivatives, have demonstrated high specificity and potency.

Species-specific amino acid differences in the CoQ Binding Site enhance the selective binding of inhibitors, with key residues like ARG265, HIS181, and LEU531 forming hydrogen bonds with inhibitors such as DSM265.^[32] Drug resistance arises primarily from mutations in critical binding pocket residues; for example, mutations like V332 and F227 in the Dd2R strain and Cys276Tyr/Cys276Phe in the DHODH gene have been linked to reduced inhibitor efficacy and higher EC₅₀ values in resistance studies.^[33]

2.1 *Pf*DHODH Structures in PDB Repository

The Protein Data Bank (PDB) presently contains 156 structures of the enzyme DHODH derived from *Plasmodium falciparum*. The structures of *Pf*DHODH deposited in the study period is listed in Table 1 and one of them has been represented in (Fig. 3a and 3b). Except for one PDB ID 6E0B, all structure contains the wild variant 3D7. The structure resolution varies between 1.96 to 3.30 angstrom. The CoQ-binding site of *Pf*DHODH exhibits significant structural flexibility, which can make it challenging to obtain consistent and high-resolution structures of the enzyme-inhibitor complex. This flexibility complicates the accurate modelling of inhibitor binding and hinders the understanding of specific interactions.^[34]

3. Review methodology

This review employs a systematic approach to analyzing the role of computational methods in the discovery of *Pf*DHODH inhibitors. A comprehensive literature search was conducted to identify relevant studies focusing on in silico techniques used in drug discovery. The selected papers were categorized into five major computational strategies: Structure-Based Pharmacophore Mapping, Quantitative Structure-Activity Relationship (QSAR), Molecular Modelling, AI-Assisted Methods, and Molecular Fractionation-Based Approaches (Fig. 4). Each category was critically examined to highlight its contributions to designing novel *Pf*DHODH inhibitors and understanding their mechanisms of action. By synthesizing data from these computational methodologies, this review aims to provide a cohesive overview of their impact on drug development, addressing a research gap in this domain.

Table 1: Crystallographic structures of *Pf*DHODH in PDB repository.

PDB ID	Ligand	Resolution (Å)
6E0B ^[34]	5-Methyl-N-(2-naphthyl) [1,2,4] triazolo[1,5-a] pyrimidin-7-amine	2.1
6GJG ^[36]	3,6-dimethyl-N-(4-(trifluoromethyl) phenyl) -(1,2) oxazolo(5,4-d) pyrimidin-4-amine	1.99
6I4B ^[33]	3-Hydroxy-1-methyl-5-((3-(trifluoromethyl) phenoxy) methyl)-1H-pyrazole-4-carboxylic acid	1.98
6I55 ^[33]	N-(2,2-Diphenylethyl)-4-hydroxy-1,2,5-thiadiazole-3-carboxamide	1.98
6VTN ^[35]	N-cyclopropyl-4-{{2-fluoro-4-(trifluoromethyl) phenyl} methyl}-3-methyl-1H-pyrrole-2-carboxamide	2.25
6VTY ^[35]	ethyl 3,5-dimethyl-4-{{4-(trifluoromethyl) phenyl} methyl}-1H-pyrrole-2-carboxylate	1.78
7KYK ^[37]	ethyl 3-methyl-4-{{4-(trifluoromethyl)-1,3-benzoxazol-7-yl} methyl}-1H-pyrrole-2-carboxylate	2.15
7KYV ^[37]	3-methyl-N-(1-(5-methylisoxazol-3-yl) ethyl)-4-(4-(trifluoromethyl) benzyl)-1H-pyrrole-2-carboxamide	2.40
7KYY ^[37]	3-methyl-N-(1-(5-methylisoxazol-3-yl) ethyl)-4-(6-(trifluoromethyl)-1H-indol-3-yl)-1H-pyrrole-2-carboxamide	2
7L0K ^[37]	3-{{(1R)-1-[(3-methyl-4-{{6-(trifluoromethyl) pyridin-3-yl} methyl}-1H-pyrrole-2-carbonyl) amino] ethyl}-1H-pyrazole-5-carboxamide	1.96
7WYF ^[38]	Ethyl 2-(naphthalen-2-ylamino)-4-oxidanylidene-furan-3-carboxylate	3.3

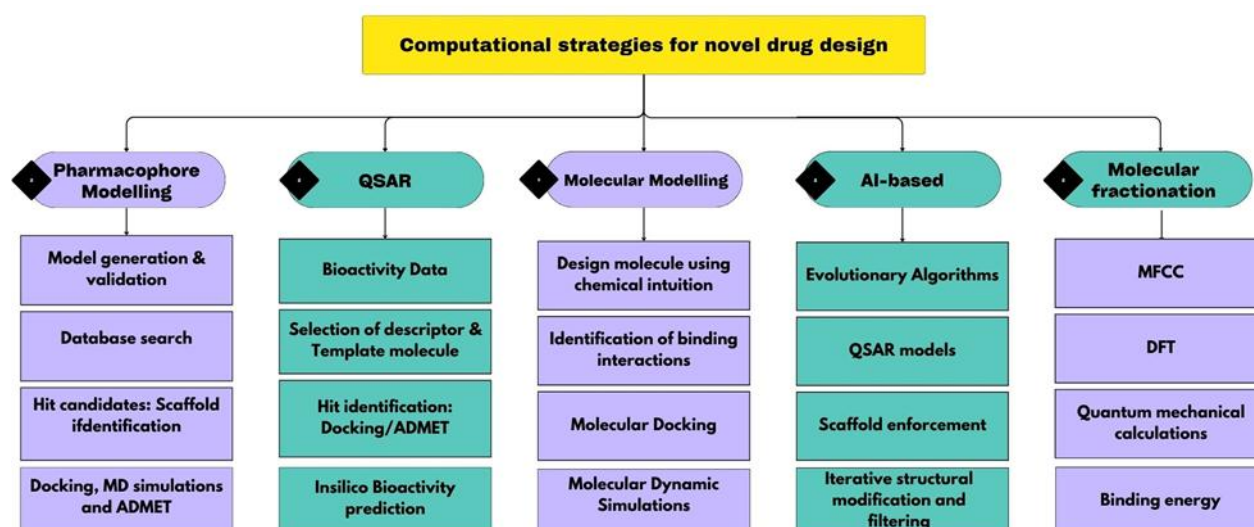


Fig. 4: Computational strategies for novel drug design.

Table 2: Summary of literature review done on the papers.

Study Objective	Method Employed	Software/Tools Used	Data Set/Data Base
SBDD based novel inhibitor design ^[39,40]	Pharmacophore, SBVS, Docking, MD Simulations, Binding Energy Calculation	Schrödinger, PyMOL, ADMET, GROMACS	ZINC, Enamine
Natural compounds based inhibitor design ^[41]	Pharmacophore Modelling, Docking, MD simulations, ADMET	Chimera 1.10.1, BioSolveIT, Schrödinger, GROMACS	SPECS natural product database
Identification of novel dual-target inhibitors ^[42]	Pharmacophore modelling, molecular docking, quantum mechanics, and MD simulations	Schrodinger	ZINC database
Novel indolyl-3-ethanone- α -thioethers' design with improved properties ^[43]	QSAR modelling, Molecular	Spartan14, Molegro, Data-Pre-treatment GUI 1.2.	Indolyl-3-ethanone- α -thioethers derivatives (31) with IC ₅₀ from literature
Novel Azetidene-2-carbonitriles' design with improved properties ^[44,45]	QSAR Modelling, Molecular docking, ADMET	Spartan14, Material Studio 8.0, Molegro Virtual Docker, SwissADME	Azetidine-2-carbonitriles derivatives (34) with EC ₅₀ (from literature)
Investigation of inhibitory mechanism of synthesized derivatives of chalcone and flavone against <i>Pf</i> DHODH ^[46,47]	Docking, MD Simulations, Binding Energy calculations	Surflex-Dock, GROMACS 4.5.5	Synthesized Compounds
Lead optimization of pyrrole series of <i>Pf</i> DHODH inhibitor through structure-based in silico methods ^[48]	Molecular docking with Wscore, WaterMap analysis, and free-energy perturbation (FEP+), Synthesis	Schrodinger	eMolecules Building Blocks 2015
Identification of novel anthocyanins as potential antimalarials ^[49]	Molecular Docking, MM-PBSA & ADMET	Schrödinger	PhytoHub
Design of 2-anilino-4-amino substituted quinazoline inhibitors ^[50]	QSAR	Data Pre-Treatment GUI 1.2	2-anilino 4-amino substituted quinazolines derivatives (45) with EC ₅₀

Study Objective	Method Employed	Software/Tools Used	Data Set/Data Base
Investigation of binding mechanism and PK of synthesized compounds ^[51] 2-hydroxyxanthone from xanthone ^[52]	Synthesis, molecular docking, ADMET, and SAR studies	Mol inspiration, admetSAR webserver, PROPKA, PyRx, This is the basis for the study ^[53]	In-house
Design of novel xanthenes based on QSAR ^[53]	QSAR, Molecular Docking, Synthesis and Bioactivity	Discovery Studio, UCSF CHIMERA, ChemOffice.	25 reported prenylated xanthone derivatives
Investigation of hydroxyxanthone derivatives as P _f DHODH inhibitors ^[54]	Molecular docking, Molecular dynamics, ADMET, MM-PBSA binding energy calculation	Avogadro, Orca, Molegro Virtual Docker software, GROMACS 2020, pkCSM server	Experimental
Investigation of the role of CF3 Pyridinyl substitution on inhibitory activity ^[55]	MD simulation	Molecular Molegro Viewer (MMV), UCSF Chimera	DSM265 and DSM421
Investigation of binding interaction of multitarget inhibitor ^[56,57]	Molecular docking, MD simulations	Schrödinger, PROPKA	MMV007571 and MMV020439
Exploration of previously reported molecules as dual target P _f DHODH inhibitors ^[58]	DFT, Molecular docking, MD simulations, ADMET	GROMACS, DFT/6-31G(d), admetSAR, Schrödinger	Derivatives
Investigate novel 2-anilino-4-amino substituted quinazolines as P _f DHODH inhibitors ^[59]	Virtual screening, Docking, Dynamic simulation, ADMET	SwissADME, Procheck, DFT/6-31G(d), MVD, Schrödinger	Derivatives
AI-based De Novo drug design ^[60]	logK _i , ADMET	AI-Driven Drug Design (AIDD)	7-aminotriazolopyrimidine Inhibitors of P _f DHODH with IC ₅₀ (from literature)
Investigation of binding characteristics and energy dynamics of the inhibitors ^[61]	MFCC, DFT	PROPKA 3., Gaussian code (G09)	DSM483, DSM557, DSM1

An analysis of the objectives, methodologies, and outcomes of these studies has been conducted, and their principal findings are summarized in Table 2.

3.1 Structure-based pharmacophore mapping

Structure-based pharmacophore mapping uses the 3D structure of a target protein or ligand-binding site to discover hydrogen bond acceptors/donors, hydrophobic areas, and aromatic rings. These features guide the design or screening of potential drug candidates by ensuring they align with the critical interaction points necessary for binding and activity.

The study by Vyas VK *et al.*^[39] aimed to develop novel inhibitors for P_fDHODH using a structure-based drug design (SBDD) approach. Starting with the co-crystal structure of P_fDHODH (PDB ID: 6I55), a five-point e-pharmacophore model was developed, which was used to conduct high-throughput virtual screening (HTVS) on the ZINC database. Model validation involved 21 active compounds from literature and 1000 decoy molecules, with feature matches

covering four ligand sites and inter-site distance constraints via the Phase module (Fig. 5a). Key design strategies included an aromatic ring with an acceptor atom, a fused heterocyclic ring with nitrogen, and a secondary amine linker connecting quinolizin-4-one to naphthalene or biphenyl rings as donor sites. Additional substituents were incorporated based on the pharmacophore. Docking studies prioritized interactions with critical residues ARG265 and HIS185 (Fig. 5b), selecting the quinolizin-4-one scaffold for further optimization.

Following a similar protocol, the study by Abdul Rahim *et al.*^[40] screened the Enamine database of 2 million compounds using the developed pharmacophore model consisting of one acceptor [A], one donor [D], two hydrophobic regions [H] and three aromatic rings [R]. It was reported that the first hydrophobic site (H9) was proximal to ASN 280 and HIS185. second hydrophobic site (H10) was near ASP169 and TYR168. While the acceptor A4 lies close to PHE 278 and LYS173 the donor D7 lies close to LEU172. Three aromatic rings R12, R13, and R14 were found in the vicinity of ILE170,

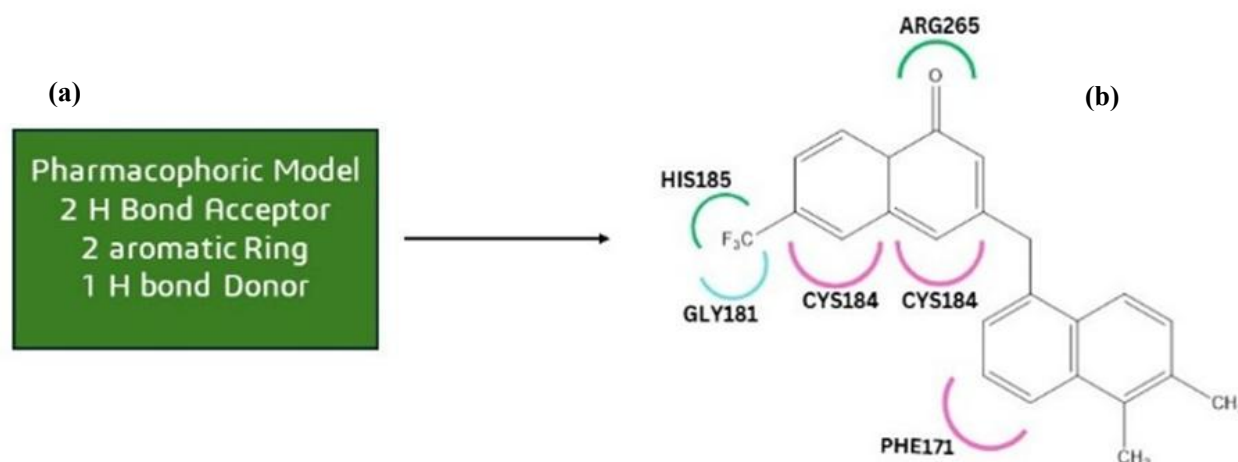


Fig. 5: a) E-pharmacophore Mapping of the model on the designed quinolizin-4-one compound Reproduced from.^[39] b) Best-designed compounds with docking interaction. **Pharmacophore features:** Aromatic ring with an acceptor atom, a fused heterocyclic ring with nitrogen, and a secondary amine linker connecting quinolizin-4-one to naphthalene or biphenyl rings as donor sites. **Critical residues:** ARG265 and HIS185.

Following a similar protocol, the study by Abdul Rahim *et al.*^[40] using docking with *Pf*DHODH (PDB ID: 7KZ4). Top screened the Enamine database of 2 million compounds using the developed pharmacophore model consisting of one acceptor [A], one donor [D], two hydrophobic regions [H] and three aromatic rings [R]. It was reported that the first hydrophobic site (H9) was proximal to ASN 280 and HIS185. While the second hydrophobic site (H10) was near ASP169 and TYR168. While the acceptor A4 lies close to PHE 278 and LYS173 the donor D7 lies close to LEU172. Three aromatic rings R12, R13, and R14 were found in the vicinity of ILE170, PHE278, and HIS185, TYR168, respectively. The compounds fitting five out of the minimum of 7 sites were further validated

compounds Z1481646084 ((4-(((5-((2-chlorophenoxy) methyl)-4-methyl-4H-1,2,4-triazol-3-yl) thio) methyl)-N-phenylbenzamide), Z24317941, and Z951873618 were identified based on docking, ADME prediction, Free binding energy calculations, and MD simulations as potential *Pf*DHODH inhibitors. Fig. 6 shows molecule (4-(((5-((2-chlorophenoxy) methyl)-4-methyl-4H-1,2,4-triazol-3-yl) thio) methyl)-N-phenylbenzamide) with key binding interactions. Prakash *et al.*^[41] developed a multicomplex-based pharmacophore using 13 high-resolution *Pf*DHODH ligand complexes with known IC₅₀ values from the PDB database.

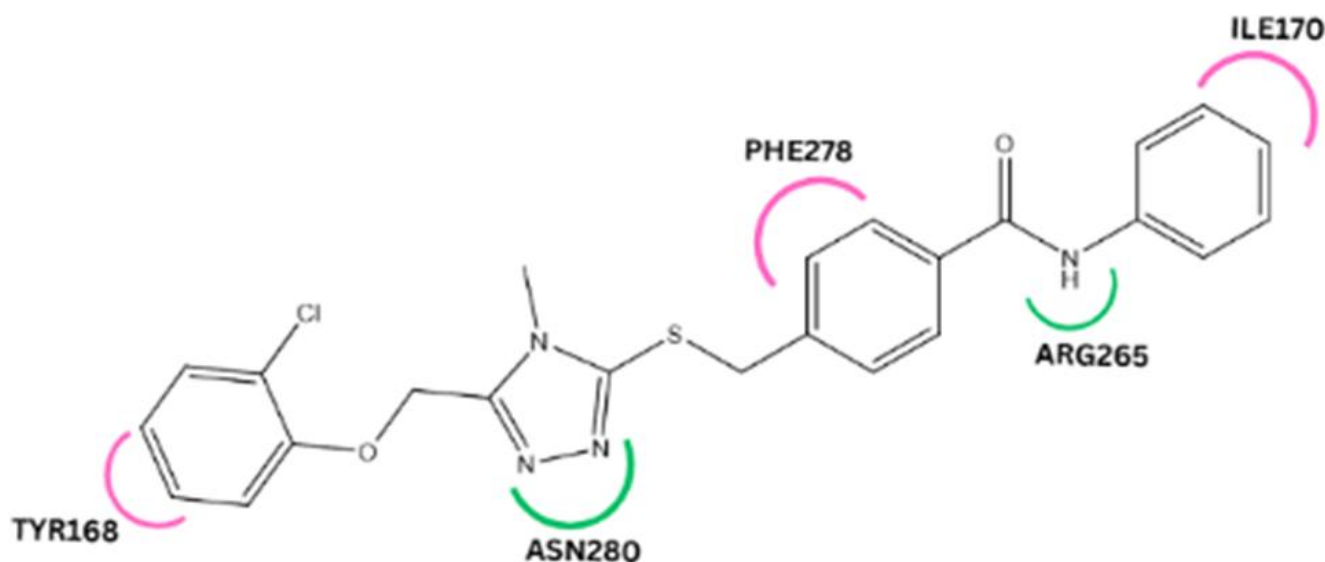


Fig. 6: 4-(((5-((2-chlorophenoxy) methyl)-4-methyl-4H-1,2,4-triazol-3-yl) thio) methyl)-N-phenylbenzamide. **Pharmacophore features:** Pharmacophore model consisting of one acceptor [A], one donor [D], two hydrophobic regions [H] and three aromatic rings [R]. **Critical residues:** ASN 280, HIS185, ASP169, TYR168, PHE 278, LYS173, LEU172, ILE170, PHE278 and HIS185, TYR168.

By superimposing receptor-ligand coordinates and using the *Pf*DHODH-Genz-669178 complex (PDB ID: 4CQ8) as a reference, they generated common pharmacophore hypotheses (CHPs) featuring H-bond acceptor/donor, hydrophobic, aromatic, and ionisable sites. Validation was performed using 59 active and 53 inactive compounds, with enrichment factor (EF) and Güner–Henry (GH) scoring to assess pharmacophore quality and hit recognition. Ligand Pharmacophore Mapping in Discovery Studio compared 813 phytochemicals from the SPECS natural product database against the pharmacophores. Further docking studies using the *Pf*DHODH-DSM422 crystal structure (PDB ID: 5FI8) identified Spec 3 (7-methoxy-1-methyl-9H-pyrido[3,4-b] indole) as a promising inhibitor. The lead molecule, Spec 3, shown in (Fig. 7), identified as potential lead molecule as it formed hydrogen bonds with key residues HIS185 and ARG265, PHE227 and VAL532, exhibited molecular stability in dynamic simulations, and demonstrated favourable drug-likeness properties.

In another study, Elamine and co-workers utilized e-

pharmacophore modelling and molecular docking to identify natural compounds targeting *Pf*DHODH and PMT, screening 76,747 ZINC database compounds and narrowing to nine candidates with promising binding affinities. Further investigations, including MM-GBSA, ADME, DFT calculations, and MD simulations, highlighted ZINC000013377887 (((R)-1,7-bis(3,4-dihydroxyphenyl)-5-hydroxyheptan-3-one)) (Fig. 8), ZINC000015113777, and ZINC000085595753 as potent dual-enzyme inhibitors interacting with key residues such as CYS175, TYR176, ILE196 ARG265, MET536^[42]

3.2 Quantitative structure activity relationship (QSAR)

QSAR modelling uses mathematical relationships between chemical structures and biological activities, leveraging statistical and machine learning methods to predict compound properties such as biological activity, toxicity, and physicochemical traits, aiding in candidate prioritization for virtual screening while minimizing experimental efforts and expediting drug discovery.

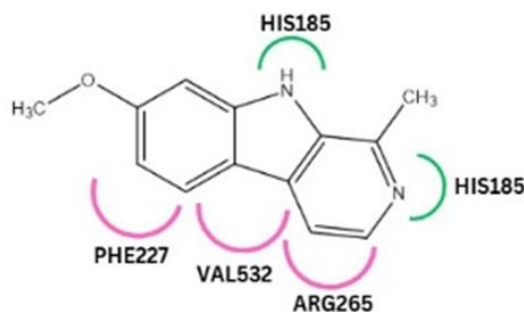


Fig. 7: Key interactions of 7-methoxy-1-methyl-9H-pyrido[3,4-b] indole (Spec 3) Reproduced from.^[41] **Pharmacophore features:** H-bond acceptor/donor, hydrophobic, aromatic, and ionisable sites. **Critical residues:** HIS185, PHE227, ARG265 and VAL 532.

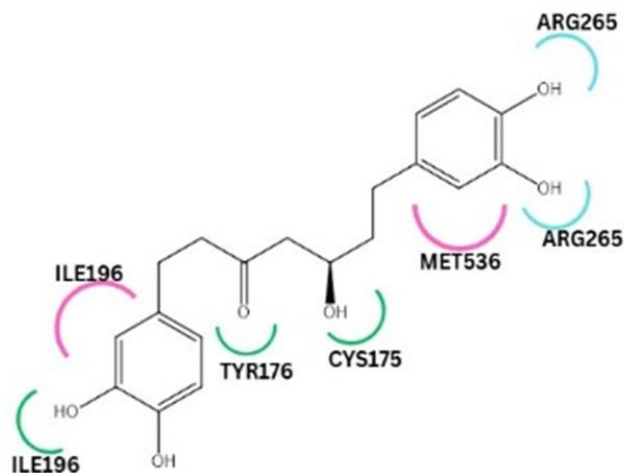


Fig. 8: Key interactions of the hit molecule: (R)-1,7-bis(3,4-dihydroxyphenyl)-5-hydroxyheptan-3-one Reproduced from.^[42] **Pharmacophore features:** one hydrogen donor (D), one hydrogen acceptor (A), two hydrophobic groups (H), and three aromatic rings (R). **Critical residues:** CYS175, TYR176, ILE196 ARG265, MET536.

Zakari *et al.*^[43] designed novel *Pf*DHODH inhibitors by analysing 31 indolyl-3-ethanone- α -thioethers derivatives. Geometry optimization and descriptor calculations were performed using DFT (B3LYP/6-311G*) and PaDEL-Descriptor. The dataset was split into training (23 compounds) and test (8 compounds) sets for model construction using Molegro Data Modeller. The optimal model showed strong predictive capability, identifying key descriptors influencing inhibitory activities. Descriptors MATS5m, VE3_Dzp, min HBa, RDF75m with positive coefficients indicated enhanced inhibition with increasing descriptor values, while AATSC8p, MLFER_BH with negative coefficients suggested increased inhibition with lower descriptor values. MLFER_BH was identified as the most significant descriptor. Docking with Molegro Virtual Docker predicted binding modes within the defined protein cavity, guiding inhibitor design. The study selected one of the molecules due to its high activity ($pIC_{50} = 7.0458$) (Fig. 9) and favourable properties for designing novel derivatives. Guided by MLFER_BH, electron-withdrawing groups like -Br, -Cl, and -NO₂ were added in the designing process. Three molecules demonstrated better antimalarial activity than chloroquine, selected compound with ($pIC_{50} = 8.2129$) showed the highest activity. It exhibited a docking score of -141.336 kcal/mol, indicating interactions with key active site residues TYR506 and SER477, CYS175, and VAL532 (Fig. 9) within the CoQ binding pocket.

Following a similar approach, researchers, Z. Ibrahim *et*

al.^[44] designed Azetidine-2-carbonitrile derivatives with enhanced activity against *P. falciparum*. A total of 34 derivatives with known structures and EC₅₀ values against the Dd2 strain were extracted from PubChem. QSAR modelling identified the descriptor SpMax2_Bhp (maximum absolute eigenvalue of the Barysz matrix weighted by polarizability) as the most influential due to its high mean effect. Increased polarizability, achieved by substituting electron-deactivating groups (F, I, Cl, SO₃H, CN, NO₂) at various positions, enhanced antimalarial activity. The shape parameter Petitjean Number also contributed, with activity rising when substituents changed from F and Cl to CF₃ or -OCH₃. From this information and considering a compound with $pEC_{50} = 8.301$ as a design template (Fig. 10a), novel derivatives were proposed. The best-proposed compound with the docking interactions is presented in (Fig. 10b). It exhibited the highest binding affinity (-177.0910 kcal/mol), outperforming other derivatives and the standard drug chloroquine.^[45]

3.3 Docking and MD Simulations for Novel *Pf*DHODH Inhibitor Design

Molecular docking and MD simulations are pivotal computational techniques in medicinal chemistry, enabling the prediction of binding interactions and stability of drug candidates with biological targets. These methods provide insights into molecular interactions, dynamic conformational changes, and energetics.

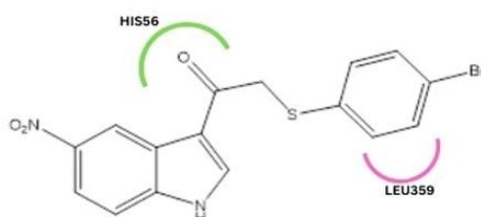


Fig. 9: Key interactions of 2-((4-bromophenyl)thio)-1-(5-nitro-1H-indol-3-yl)ethan-1-one obtained by replacing Cl by NO₂ Reproduced from.^[43] **Database:** 31 indolyl-3-ethanone- α -thioethers derivatives **Descriptor used:** PaDEL-Descriptor **Key descriptors influencing inhibitory activities:** MATS5m, VE3_Dzp, min HBa, RDF75m, AATSC8p.

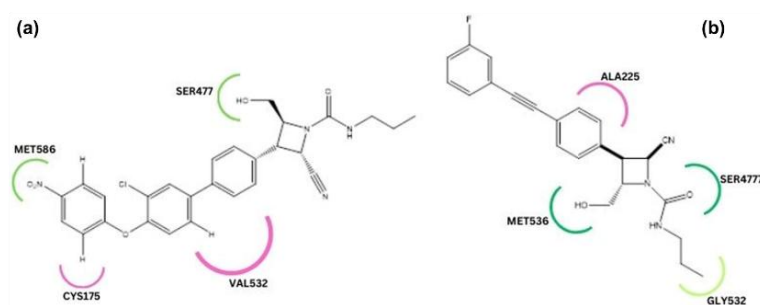


Fig. 10: a) Template molecule- (2S,3S,4R)-3-(3'-chloro-4'-(4-nitrophenoxy)-[1,1'-biphenyl]-4-yl)-2-cyano-4-(hydroxymethyl)-N-propylcyclobutane-1-carboxamide. b) Key interactions on (2S,3S,4R)-2-cyano-3-(4-((3-fluorophenyl)ethynyl)phenyl)-4-(hydroxymethyl)-N-propylazetidine-1-carboxamide Reproduced from.^[45] **Database:** Azetidine-2-carbonitrile derivative **Descriptor used:** SpMax2_Bhp as the most influential descriptor due to its high mean effect.

Chalcones and flavones, known for their structural versatility and ease of synthesis, gain enhanced pharmacological properties when integrated with 1,2,3-triazole scaffolds, making them effective pharmacophores for antimicrobial and antimalarial applications.^[46] Mahalakshmi *et al.*^[47] designed 25 triazole-linked chalcone-flavone hybrids, incorporating substitutions like dimethoxy, hydroxyl, chlorine, and fluorine for improved pharmacological activity. In silico studies revealed strong binding with the target protein (PDBID: 4CQ9) for the most active ligand, (2E)-3-(4-([1-(3-chloro-4-fluorophenyl)-1H-1,2,3-triazol-4-yl]methoxy)-3-methoxyphenyl)-1-(2-hydroxy-4,6-dimethoxyphenyl) prop-2-en-1-one shown in Fig. 11. This study identified that modifications with functional groups such as methoxy and fluorine enhanced interactions with key residues. The most active ligand formed nine hydrogen bonds with key residues, including SER529, SER477, PHE278, and LYS429 and THR249, highlighting its potential as an effective inhibitor. Docking results were supported by MD simulations (40,000 ps), showing stable RMSD values and minimal structural deviations. MD simulations demonstrated the compound's superior stability. RMSF analysis confirmed minimal residue fluctuations, and lower Rg values (1.8–1.9 nm) indicating better protein-ligand compactness.^[47]

Although DSM265 exhibited strong efficacy, its teratogenicity and testicular toxicity prevented further clinical development, while still validating DHODH as a viable malaria prophylaxis target. DSM502 showed in vivo efficacy but required optimization due to lower metabolic stability and CYP inhibition. Building on this, Palmer *et al.*^[48] proposed novel pyrrole-derived DHODH inhibitors through structure-based computational lead optimization. The study thoroughly examined the effects of replacing benzyl and cyclopropylamine with more potent substituents. Accordingly, commercial precursor libraries (eMolecules Building Blocks 2015) were docked into the binding site using WScore, and the binding pocket was examined with Water Map to elucidate binding interactions.

The most well-docked complexes were further assessed using free-energy perturbation (FEP+) to forecast their capability to inhibit DHODH. Retrospective validation with previously reported inhibitors and newly obtained X-ray structures refined the models, leading to the identification of seven new pyrrole analogue-DHODH complexes. The study identified two compounds DSM705 and DSM873 (Fig. 12a and 12b), featuring a cyclopropyl group on the bridging carbon possibly responsible for eliminated time-dependent CYP inhibition, with better physiochemical and pharmacokinetic features than DSM 265. This computational modelling approach facilitated the prioritization of compounds for synthesis.

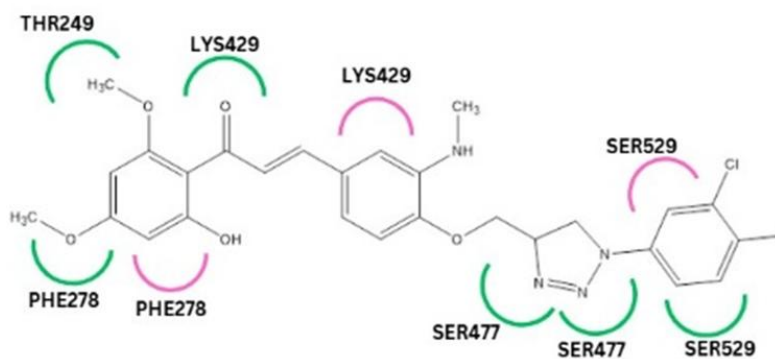


Fig. 11: Interactions on the hit molecule: (2E)-3-(4-([1-(3-chloro-4-fluorophenyl)-1H-1,2,3-triazol-4-yl]methoxy)-3-methoxyphenyl)-1-(2-hydroxy-4,6-dimethoxyphenyl)prop-2-en-1-one Reproduced from.^[47] **Database:** 25 triazole-linked chalcone-flavone hybrids **Key Residues:** SER529, SER477, PHE278, and LYS429 and THR249 **Key highlight:** Functional groups such as methoxy and fluorine enhanced interactions with key residues.

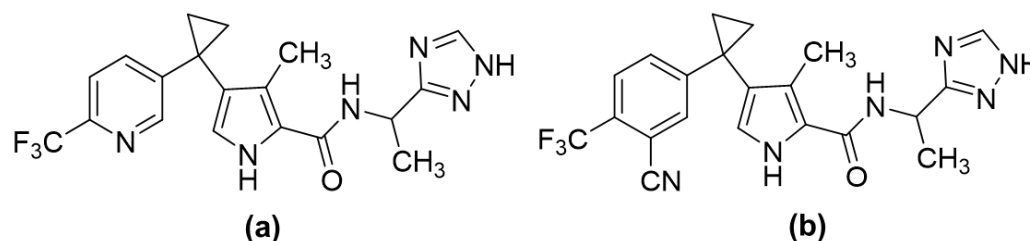


Fig. 12: a) DSM705. b) DSM873. **Key highlight:** A cyclopropyl group on the bridging carbon is possibly responsible for eliminated time-dependent CYP inhibition, with better physiochemical and pharmacokinetic features than DSM 265.

Study by Afolabi *et al.*^[49] analysed Phytohub anthocyanins compounds using computational methods, including as possible inhibitors using computer-aided molecular electrostatic potential analysis, pharmacological assessments, modeling, including molecular docking, MM/GBSA and molecular docking. The pharmacokinetic properties were calculations, and ADMET screening of key Plasmodium assessed using ADMET SAR and Molinspiration tools. *falciparum* enzymes (*PfDHODH*, *PfLDH*, and *PfDHFR*). Five top-scoring anthocyanins with strong binding affinities to critical sites MET 536, CYS175, CYS 184, ARG 265 were identified. Fig. 13 shows the best molecule with key binding with residues. The paper highlighted the role of structure-based modelling in discovering malaria inhibitors from natural products.^[49]

Quinazolin-2,4-diones are valuable structural cores in medicinal and pharmaceutical chemistry, particularly when combined with nitrogen-containing heterocycles like azetidinone, pyrazole, and oxazole. The study by Ibrahim *et al.*^[50] focussed on synthesizing nitrogen heterocyclic systems linked to the quinazoline-2,4-dione scaffold via acetyl/amide linkages at the nitrogen N-1 position as shown in Fig. 14. The study investigated binding mechanisms of synthesized

compounds using computational methods, including electrostatic potential analysis, pharmacological assessments, and molecular docking. The pharmacokinetic properties were assessed using ADMET SAR and Molinspiration tools. Additionally, molecular interactions, such as hydrogen bonding and π - π stacking, were analyzed, and the binding energies of the synthesized compounds were compared to those of chloroquine as the reference drug. The compound with the highest binding energy (-12 kcal/mol) is depicted in Fig. 15, highlighting its key interactions, including hydrogen bonds with PHE278, LYS429, ILE508, and GLY506, along with π - π stacking with TYR528. The study concluded that the heterocyclic core structures combined with acetyl/amide linkages could enhance the drug activity.^[51]

Aminatie *et al.*^[52] reported that 2-hydroxyxanthone derivatives, as shown in Fig. 16a, have enhanced antimalarial activity while Syahri *et al.*^[53] showed that adding hydroxyl groups and substituents like phenyl, nitro, sulphate, and chloro to these compounds further boosts efficacy.

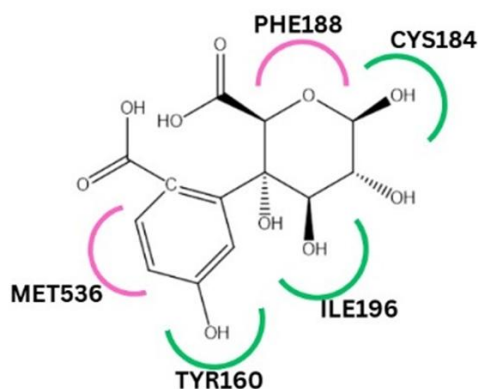


Fig. 13: Key interactions of (2S,3S,4R,5R,6R)-3-(1-carboxy-3-methylcyclohexa-2,4-dien-1-yl)-3,4,5,6-tetrahydroxytetrahydro-2H-pyran-2-carboxylic acid mentioned in paper Reproduced from.^[49] **Database:** Phytohub anthocyanins **Key residues:** MET 536, CYS175, CYS 184, ARG 265.

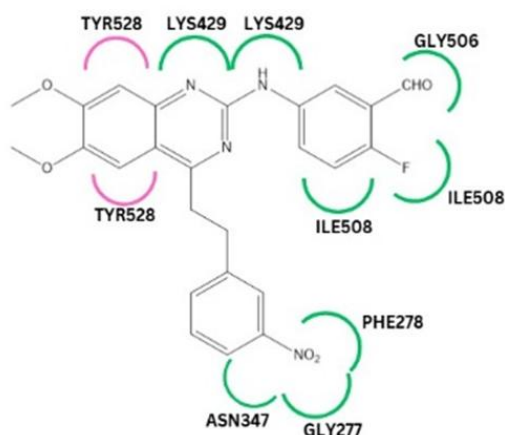


Fig. 14: Key interactions on N4-benzyl-N2-(4-fluorophenyl)-6,7-dimethoxyquinazoline-2,4-diamine Reproduced from.^[50]

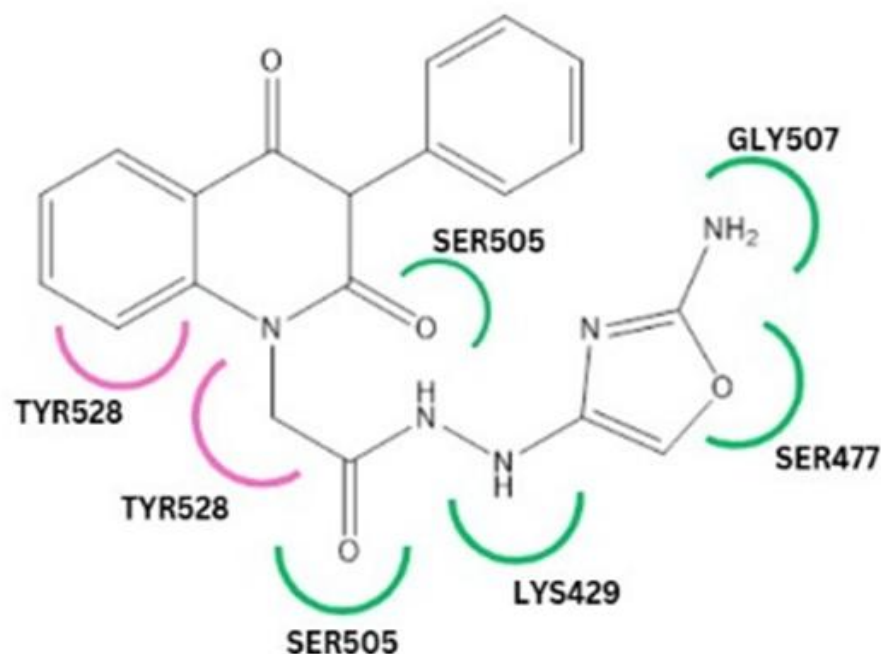


Fig. 15: Key interactions on N'-(2-aminoxazol-4-yl)-2-(2,4-dioxo-3-phenyl-3,4-dihydroquinazolin-1(2H)-yl)acetohydrazide. Reproduced from [51]. **Database:** Nitrogen heterocyclic systems linked to the quinazolinone-2,4-dione scaffold via acetyl/amide linkages at the nitrogen N-1 position. **Key residues:** MET 536, CYS175, CYS 184, ARG 265 **Key Highlight:** Heterocyclic core structures combined with acetyl/amide linkages could enhance the drug activity.

Aminatie *et al.* [52] reported that 2-hydroxyxanthone sulphate, and phenyl substituents with *Pf*DHODH PDB ID:1J3I, identified one compound X14, as the most promising inhibitor. The compound formed strong interactions with critical residues HIS185, ARG265, and TYR168 (Fig. 16b) at the *Pf*DHODH active site, outperforming the native ligand A26 and chloroquine. MD simulations confirmed the stability of three of the compounds, with RMSD values around 2.5 Å, and MM-PBSA calculations demonstrated X14's superior binding affinity. Moreover, X14 and other derivatives met Lipinski's rule and exhibited favorable ADMET properties, making them strong candidates for antimalarial drug development. [54]

Despite promising results from molecular docking and QSAR analysis, further research was needed into their binding poses, inhibition mechanisms, and stability. For this, molecular docking, MD simulations, MM-PBSA binding energy calculations, and ADMET predictions were done by Latifah *et al.* The study included molecular docking and MD simulations on hydroxyxanthone designed derivatives with chloro, nitro, sulphate, and phenyl substituents with *Pf*DHODH PDB ID:1J3I, identified one compound X14, as the most promising inhibitor. The compound formed strong interactions with critical residues HIS185, ARG265, and TYR168 (Fig. 16b) at the *Pf*DHODH active site, outperforming the native ligand A26 and chloroquine. MD simulations confirmed the stability of three of the compounds, with RMSD values around 2.5 Å, and MM-PBSA calculations demonstrated X14's superior binding affinity. Moreover, X14 and other derivatives met Lipinski's rule and exhibited favorable ADMET properties, making them strong candidates for antimalarial drug development. [54]

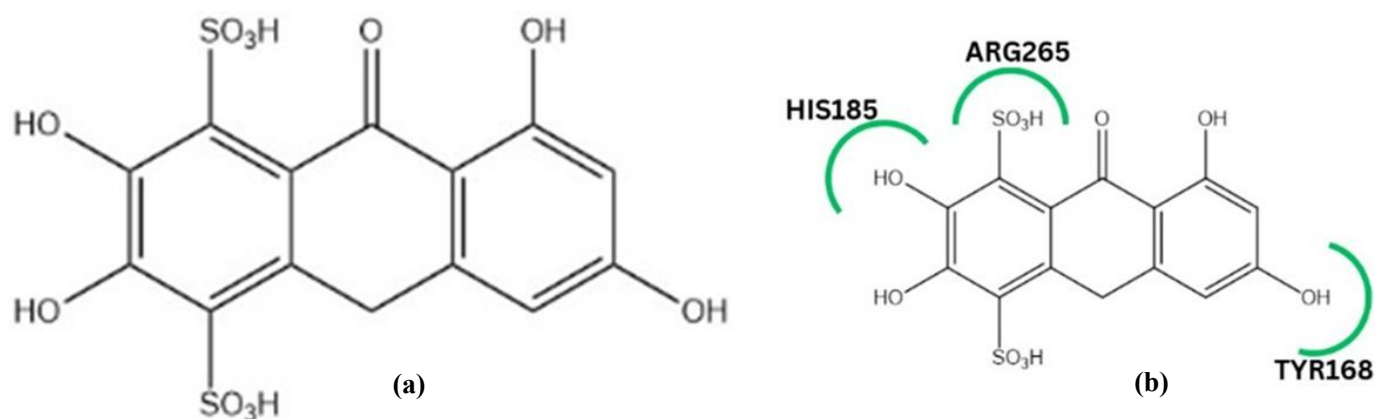


Fig. 16: a) 3,6-dihydroxy-9H-xanthen-9-one Reproduced from [52,53] b) 2,3,6,8-tetrahydroxy-9-oxo-9H-xanthene-1,4-disulfonic acid Reproduced from [54]. **Database:** 2-hydroxyxanthone derivatives. **Key residues:** HIS185, ARG265, and TYR168. **Key Highlight:** Adding hydroxyl groups and substituents like phenyl, nitro, sulphate, and chloro to these compounds further boosts the efficacy.

DSM421, depicted in Figure 16, is a structural analogue of DSM265 obtained by substituting the SF₅-aniline moiety with a CF₃-pyridinyl group. This modification enhances aqueous solubility, reduces metabolic clearance, and results in higher plasma exposure and a longer predicted half-life, while also simplifying synthetic accessibility—collectively improving its suitability for clinical development against *Pf*.^[48] To investigate DSM421's improved inhibitory efficacy, molecular dynamics simulations, and MM/PBSA-based free binding energy assessments were performed on X-ray crystal structures of *Pf*DHODH complexed with DSM421 and DSM265. It was observed that the DSM421 demonstrates superior inhibitory potency over DSM265 against *Pf*DHODH, driven by enhanced residue rigidity and stable binding interactions. RMSD and RMSF analyses indicated tighter residue interactions while free energy calculations reveal that DSM421's higher binding affinity (6.64 kcal/mol) is due to increased van der Waals and electrostatic interactions. Key interactions include halogen bonding and π - π stacking with SER236 and PHE188 (Fig. 17) from DSM421's CF₃-pyridinyl group, as compared to DSM265's SF₅-aniline, leading to differences in their properties. These findings thus highlight structural differences influencing binding efficiency, offering insights into the rational design of potent *Pf*DHODH inhibitors for improved malaria therapy.^[55]

A similar study by Rawat and team^[56] investigated the binding mechanism to get insights into residue interactions and pharmacophoric features of previously published work by Gilson and co-workers.^[57] In this work, two powerful NPP (new permeability pathway) inhibitors, MMV007571 and MMV020439, the thiophene-2-carboxamides, showed good parasite inhibition in NLuc tests, with EC₅₀ values of 367 nM and 222 nM, respectively. In vitro studies showed that MMV007571 inhibited *Pf*DHODH (Fig. 15), while metabolic profiling showed a secondary phenotype that increased intracellular N-carbamoyl-aspartate and dihydroorotate levels after 6 hours. The compound showed inhibition of *Pf*DHODH directly and indirectly via the cytochrome bc1 complex, similar to Atovaquone. This prompted an investigation to look into their binding mechanisms by Rawat and co-workers. Docking studies of MMV007571 (Fig. 18) exhibited efficient π -stacking with PHE188 and better binding efficiency due to its smaller size and proper aromatic ring placement, while MMV020439 performed better in cytochrome bc1 complex docking due to hydrophobic interactions in the larger Q₀ site. Additional MD simulations on MMV007571 revealed alterations in the N-terminal α -helix domain of *Pf*DHODH, which controls ubiquinone entry. Ligand-bound *Pf*DHODH complexes had smaller gate sizes (16-18 Å) than the native model (24 Å), indicating a transition from open to closed states. Analysis of cofactor binding revealed diminished H-bond contacts with flavin mononucleotide (FMN) in ligand-bound models, disrupting cofactor-dependent substrate oxidation and enzymatic activity. MMV007571 exhibited mixed-type inhibition by inducing conformational changes in key domains, disrupting ubiquinone and FMN interactions. Structural insights highlight potential modifications for developing potent multitarget antimalarial inhibitors^[56]

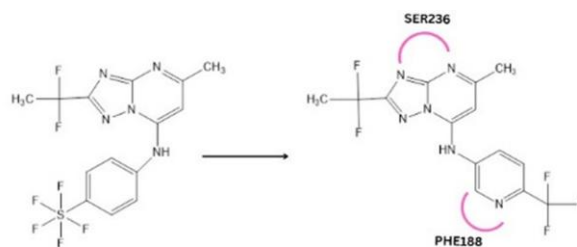


Fig. 17: Modification of DSM265 to DSM421 Reproduced from.^[55] **Database:** DSM265 **Key residues:** SER236 and PHE188 **Key Highlight:** Structural differences influencing binding efficiency, offering insights into the rational design of potent *Pf*DHODH inhibitors for improved malaria therapy.

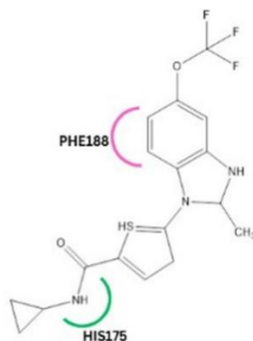


Fig. 18: MMV007571 (N-cyclopropyl-2-(2-methyl-5-(trifluoromethoxy)-1H-benzo[d]imidazol-1-yl)-3H-thiophene-5-carboxamide) with key binding interactions Reproduced from.^[56] **Database:** MMV library **Key residues:** HIS175 and PHE188 **Key Highlight:** Smaller size and proper aromatic ring placement resulted in better binding efficiency

Two Azabenzimidazole derivatives, active against diseases like malaria and trypanosomiasis, were studied for *Trypanosoma brucei* TryR and *Pf*DHODH inhibition.^[58] In an investigatory study, aimed to address drug resistance in co-infections by Oluwafemi *et al*, involving DFT optimization, molecular docking (PDBID: 4NEV and 6I55), MD simulations, ADMET, and drug-likeness analysis, bioactivity and pharmacokinetics. The top hit molecule N, N'-bis[2-(5-bromo-7-azabenzimidazol-1-yl) acetyl]-1,2-ethylenediamine demonstrated a binding score of -6.724 kcal/mol with *Pf*DHODH through hydrogen bonding (HIS185 and TYR528) (Fig. 18) and π - π stacking, outperforming the co-crystallized ligand's score of -6.134 kcal/mol. Similarly, the next top-hit molecule formed a hydrogen bond with HIS185. Exhibiting favorable ADME properties and maintaining RMSD values below 0.135 nm, the first compound in (Fig. 19) demonstrated excellent stability within the *Pf*DHODH binding pocket and was identified as an effective *Pf*DHODH inhibitor.^[58]

3.4 Artificial Intelligence-based Novel Drug Design Program

A unique application of AI-based methods AIDD is an advanced computational drug discovery tool that integrates molecular evolution with PBPK simulations, optimizing activity and pharmacological properties while ensuring chemical validity. It employs evolutionary algorithms, QSAR models, ADMET risk assessment (Fig. 20), and SMARTS-based scaffold enforcement, allowing user-defined parameters to refine drug candidates through iterative structural modifications and filtering processes. AIDD generates drug candidates by transforming parent molecules through weighted selection, filtering for scaffold consistency, and iteratively optimizing pharmacokinetic properties and synthetic feasibility. The process includes evolutionary exploration, Pareto optimization, and post-processing refinements, making AIDD a robust tool for de novo drug discovery and lead optimization in pharmaceutical research.^[60]

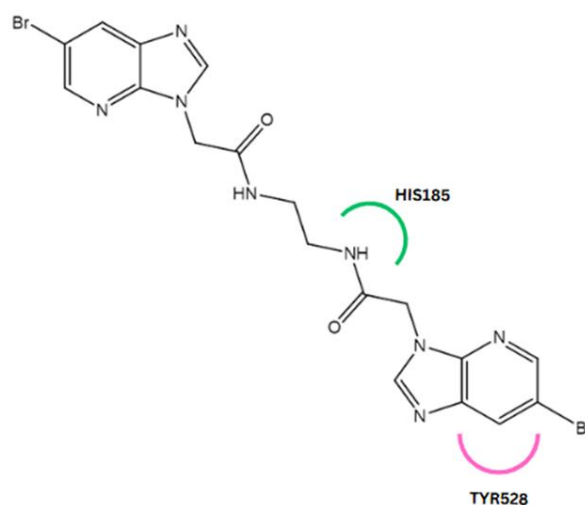


Fig. 19: Key interactions of the hit molecule: N, N'-bis[2-(5-bromo-7-azabenzimidazol-1-yl) acetyl]-1,2-ethylenediamine. Reproduced from.^[58] **Data Used:** Azabenzimidazole derivatives **Key residues:** HIS185 and TYR526.

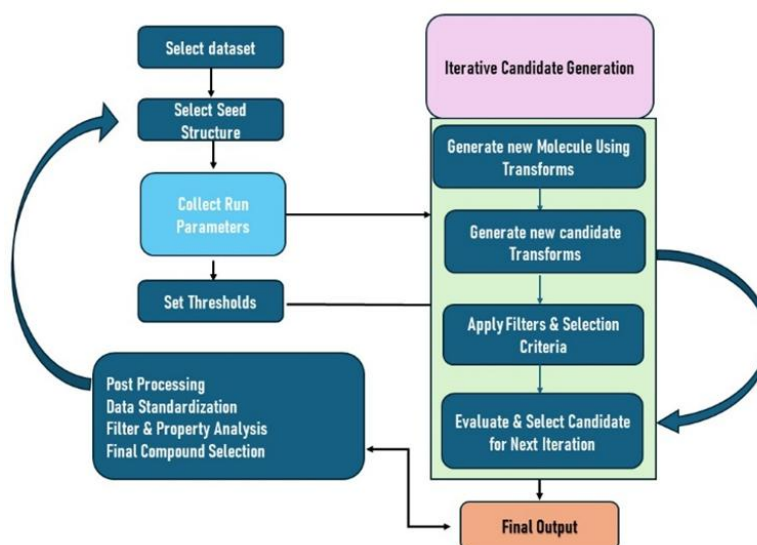


Fig. 20: The AI-driven Drug Design (AIDD) platform: an interactive multi-parameter optimization system integrating molecular evolution with physiologically based pharmacokinetic simulations. Reproduced from.^[60]

Applying AIDD (Artificial Intelligence-driven Drug Design) to a dataset of TzP *Pf*DHODH inhibitors, the system successfully generated structurally diverse candidates using a minimally substituted DSM12 scaffold as a seed molecule. Across three replicates, AIDD identified at least 35 literature-based Triazolopyrimidine (TzP)s, some of which underwent rigorous selection, demonstrating the program's ability to generate novel yet relevant drug-like molecules. Fig. 21 demonstrates some of the structures designed by the program had been synthesized.

3.5 Molecular fractionation

The study by Lima Costa *et al.*, was focused on individual amino acid interactions for accurate and affordable insights into protein-ligand dynamics using the MFCC combined with quantum DFT calculations on DSM483, DSM557, and DSM1 complexes. Protein structures retrieved from PDB repository (PDB ID: 6VTY, 6VTN, 3I65, and 6E0B) were fragmented into individual amino acids by breaking peptide bonds and adding capping groups to preserve the local chemical environment and avoid dangling bonds. Quantum mechanics-based energy calculations were performed using DFT with the B97D functional, suitable for noncovalent interactions. The 6-311+G (d, p) basis set was used for electronic wave function

representation, and the conductor-like polarizable continuum model simulated the surrounding electrostatic environment with dielectric constants of 10 and 40. Binding energy convergence was evaluated by varying the ligand-binding pocket radius.^[61] Investigations concluded the DSM1's (Fig. 22a) resilience to C276F mutation because of its highest interaction energy. Key residues, including ARG265, CYS184, PHE188, VAL532, LEU172, and PHE227, were identified as critical binding sites (Fig. 22b)

3.6 Recent developments

With the developments in DSM265 core halted due to long-term toxicity concerns, recently researchers used computational tools, including free energy perturbation (FEP+), to design potent and selective pyrazole-based DHODH inhibitors via scaffold hopping from a pyrrole-based series. The lead compound, DSM1465, showed superior potency, improved pharmacokinetics, and better ADME properties than DSM265, with promising oral activity in a humanized mouse model. These improvements support its potential for once-monthly chemoprevention in malaria-endemic regions. Another compound, referred to as "82" (Fig.23), has also emerged as a strong preclinical candidate. Further safety, resistance, and pharmacokinetic studies are

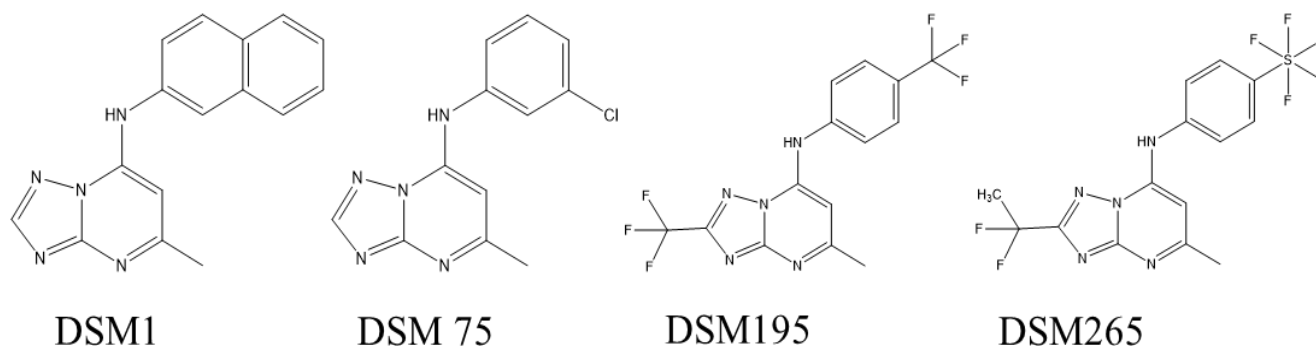


Fig. 21: Some of the TzPs identified by AIDD.

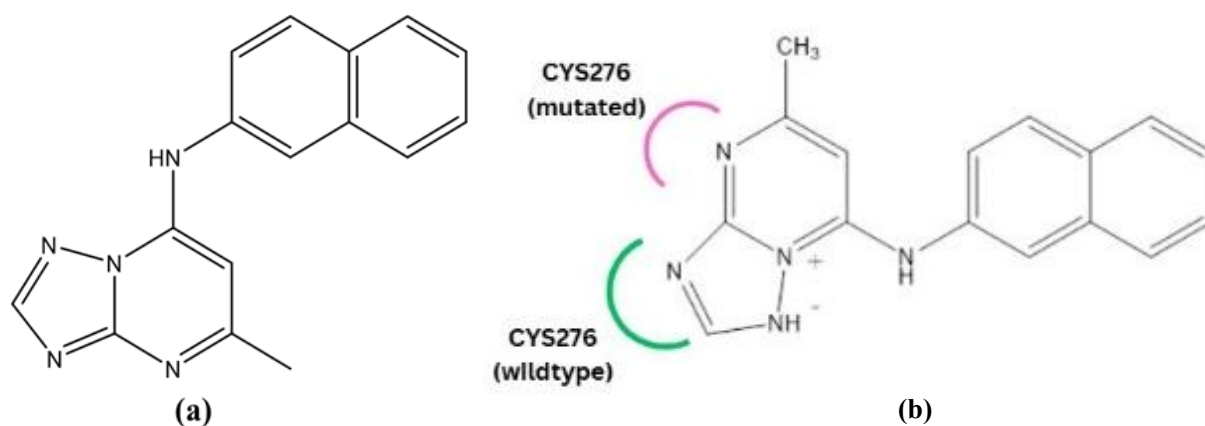


Fig. 22: a) DSM1 and b) Residues CYS276 (wild type) and PHE276 (mutated) with the lowest interaction distance to DSM1 and computed energy value. Reproduced from.^[61] **Database:** DSM483, DSM557, and DSM1 **Key residues:** ARG265, CYS184, PHE188, VAL532, LEU172, and PHE227 **Key Highlight:** Investigations concluded the DSM1's resilience to C276F mutation because of its highest interaction energy.

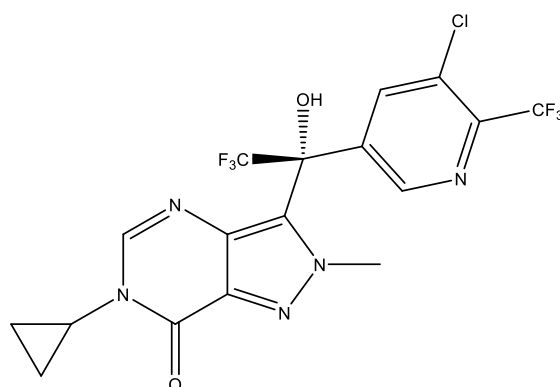


Fig. 23: (R)-3-(1-(5-chloro-6-(trifluoromethyl) pyridin-3-yl)-2,2,2-trifluoro-1-hydroxyethyl)-6-cyclopropyl-2-methyl-2,6-dihydro-7H-pyrazolo[4,3-d] pyrimidin-7-one (Compound 82).

needed to confirm their suitability for clinical use.^[62]

Another recent study explored the antimalarial potential of 7-methoxy-8-(3-methylbut-2-en-1-yl) chroman-4-one 5,7,8-prenylated flavonoids from the neem plant (*Azadirachta indica*) trihydroxy-2-(4-hydroxy-3-(3-methylbut-3-en-1-yl) phenyl) chroman-4-one respectively, demonstrated strong binding, their ability to inhibit three key *Plasmodium falciparum* stability, and favorable pharmacokinetic properties. F2 showed excellent fit and pharmacokinetics, while F6 displayed notable and *PfDHODH*. Molecular docking and dynamics simulations stability. The findings suggest both compounds, particularly F6, are promising antimalarial candidates requiring further interaction with essential amino acids. Compounds F2 (Fig. 24) validation through laboratory studies.^[63]

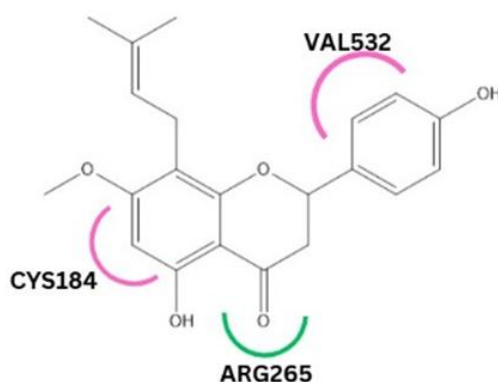


Fig. 24: Key interactions of the top hit molecule F2: (5-hydroxy-2-(4-hydroxyphenyl)-7-methoxy-8-(3-methylbut-2-en-1-yl) chroman-4-one).

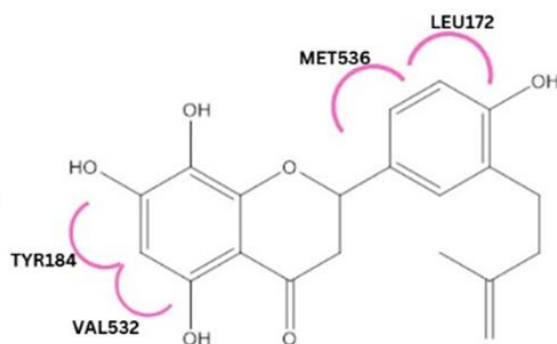


Fig. 25: Key interactions of the top hit molecule F6: 5,7,8-trihydroxy-2-(4-hydroxy-3-(3-methylbut-3-en-1-yl)phenyl)chroman-4-one).

Recent work by other researchers presents a green, solvent-free synthesis method for phenylamino naphthoquinone derivatives (compounds 1–12) using silica gel as a solid acid support. These compounds were evaluated for antibacterial and antiplasmodial activity using in vitro and in silico methods. Six compounds (especially 1, 3, and 5) showed strong antibacterial activity against *Staphylococcus aureus*, outperforming standard antibiotics like cefazolin and cefotaxime. Compounds 1 and 3 also exhibited potent antiplasmodial activity against both chloroquine-sensitive and chloroquine-resistant *Plasmodium falciparum* strains, with compound 3 being particularly effective. Docking and ADMET predictions supported their potential as drug candidates. Overall, this green synthesis approach yielded promising antibacterial and antimalarial agents, especially compound 3 identified as 2-(o-tolylamino)naphthalene-1,4-dione^[62] (Fig. 26). Yet another published work reports the synthesis and structural characterization of two Schiff base ligands, and their transition metal complexes with Co(II), Ni(II), Cu(II), and Zn(II). Structural analysis confirmed octahedral geometry and stable, non-electrolytic complexes. In vitro tests showed that Cu(II) (compound 9) and Zn(II) (compound 10) complexes exhibited the strongest antimalarial and antimicrobial activity, with low IC₅₀ values against *Plasmodium falciparum* and notable efficacy against *Candida albicans* and *E. coli*. Compounds 5 and 6 also demonstrated significant antioxidant activity. The model of the compound is represented in Fig. 27. Molecular docking studies supported these findings, showing that compounds 2 and 7–10 bind effectively to dihydroorotate dehydrogenase and sterol 14- α demethylase, key enzymes in parasite and microbial metabolism. In silico ADMET analysis confirmed favorable oral drug-like properties. Overall, the research highlights the promise of Schiff base metal complexes, especially Cu(II) and Zn(II) derivatives, as affordable and potent drug candidates for parasitic and microbial diseases.^[63]

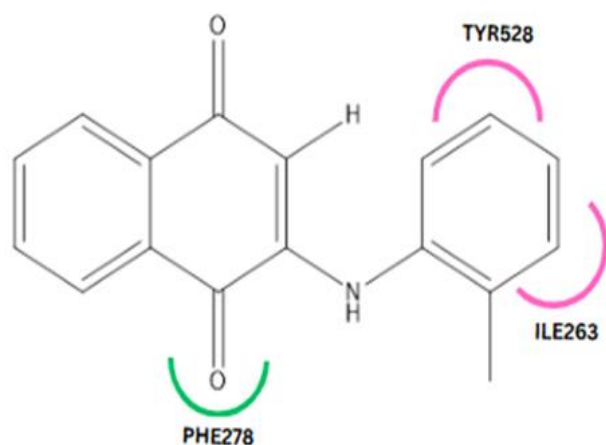


Fig. 26: Key interactions of top hit Compound 3: 2-(o-tolylamino)naphthalene-1,4-dione.

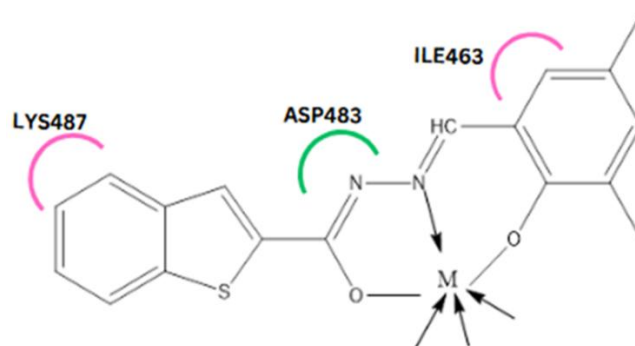


Fig. 27: Molecular scaffold representing the core structure used in the design of derivative compounds.

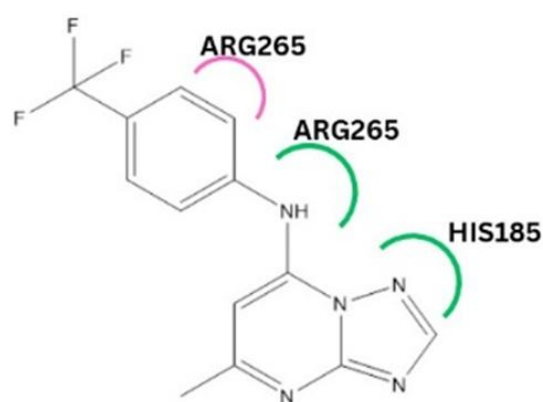


Fig. 28: Key interactions of top hit molecule DSM74.

A further recent study explores the antimalarial potential of anthraquinone compounds derived from *Morinda lucida*, a plant widely used in African traditional medicine for malaria treatment. Using molecular docking and ADMET analysis, the compounds showed strong binding affinity to *Pf*DHODH, with docking scores ranging from -9.8 to -8.6 kcal/mol—comparable to the standard compound DSM74 (Fig. 28). Key interactions occurred with residues LYS-229 and SER-477. ADMET predictions indicated excellent pharmacokinetic properties and low toxicity, suggesting these compounds are safe and bioavailable. The findings support the potential of *M. lucida* anthraquinones as novel antimalarial drug candidates. However, further biological and in vitro validation studies are needed to confirm their therapeutic efficacy.^[66]

4. Conclusion

Computational methods have played a crucial role in the discovery and optimization of *Pf*DHODH inhibitors, offering valuable insights into the development of next-generation antimalarial drugs. Techniques such as molecular docking, virtual screening, and machine learning have greatly accelerated the identification of potent therapeutic candidates. Despite promising initial results, DSM265 exhibited limitations in clinical settings due to low potency, short half-life, and emerging parasite resistance. To overcome these

challenges, computational approaches were employed in the design of DSM421, improving upon DSM265's shortcomings. Pharmacophore mapping has been instrumental in identifying key structural features in *Pf*DHODH drug candidates, enabling the discovery of novel scaffolds with enhanced properties. Additionally, QSAR techniques have been applied to develop enzyme-targeted inhibitors such as indolyl-3-ethanone- α -thioethers and azetidine-2-carbonitrile derivatives, which demonstrate improved efficacy. Molecular hybrid approaches have also been explored, leveraging existing molecular scaffolds with drug potential to design more effective candidates. Molecular docking and MD simulations have been essential in studying molecular-protein interactions, while a unique study utilized MFCC to assess the effectiveness of DSM derivatives in mutant *Pf*DHODH. Furthermore, an AI-driven program successfully generated novel molecules using scaffolds as input, highlighting the potential of artificial intelligence in drug discovery.

Computational techniques have indeed advanced drug discovery, but challenges persist, including limited validated datasets, restricted data access, and the need for robust open-source tools. Moving forward, refining computational methodologies and integrating experimental validation will be essential for translating these discoveries into effective clinical treatments, advancing efforts against drug-resistant malaria.

Acknowledgments

We would like to acknowledge Amrita Vishwa Vidyapeetham for its support and encouragement on preparation of this work. Funding: The authors declare that there was no funding received for this project.

Conflict of Interest

The authors declare that they have no known competing financial interests or personal relationships that could have appeared to influence the work reported in this paper.

Supporting Information

Not applicable.

Declaration of generative AI and AI-assisted technologies in the writing process

During the preparation of this work, the authors used Quill Bot and Grammarly in order to enhance the clarity, accuracy, and overall quality of the text. After using this tool/service, the authors reviewed and edited the content as needed and take full responsibility for the content of the publication.

CRedit Statement

Thejus Varghese Thomas: Writing - Original draft, Conceptualization, Data curation, Methodology, Investigation. **Amrita Thakur:** Review and Editing, Data curation, Supervision, Validation, Formal analysis, Methodology. **Anil Kumar S:** Data Curation, Editing, Supervision, Validation,

Final draft.

References

- [1] S. Jarcho, Laveran's discovery in the retrospect of a century, *Bulletin of the History of Medicine*, 1984, **58**, 215–224.
- [2] R. Carter, K. N. Mendis, Evolutionary and historical aspects of the burden of malaria, *Clinical Microbiolounvegy Reviews*, 2002, **15**, 564–594, doi: 10.1128/CMR.15.4.564-594.2002.
- [3] H. O. Lobel, C. C. Campbell, I. K. Schwartz, J. M. Roberts, Recent trends in the importation of malaria caused by *Plasmodium falciparum* into the United States from Africa, *Journal of Infectious Diseases*, 1985, **152**, 613–617, doi: 10.1093/infdis/152.3.613.
- [4] R. A. Bayoumi, The sickle-cell trait modifies the intensity and specificity of the immune response against *P. falciparum* malaria and leads to acquired protective immunity, *Medical Hypotheses*, 1987, **22**, 287–298, doi: 10.1016/0306-9877(87)90193-9.
- [5] A. Björkman, P. A. Phillips-Howard, The epidemiology of drug-resistant malaria, *Transactions of the Royal Society of Tropical Medicine and Hygiene*, 1990, **84**, 177–180, doi: 10.1016/0035-9203(90)90246-b.
- [6] George S, Joy TM, Kumar A, Panicker KN, George LS, Raj M, Leelamoni K, Nair P. Prevalence of Neglected Tropical Diseases (Leishmaniasis and Lymphatic Filariasis) and Malaria Among a Migrant Labour Settlement in Kerala, India. *J Immigr Minor Health*, 2019 June **21**(3), 563-569, doi: 10.1007/s10903-018-0767-9.
- [7] D. F. Clyde, Drug resistance of malaria parasites in Tanzania, *East African Medical Journal*, 1966, **43**, 405–408.
- [8] N. J. White, S. Pukrittayakamee, T. T. Hien, M. A. Faiz, O. A. Mokuolu, A. M. Dondorp, *Malaria, The Lancet*, 2014, **383**, 723–735, doi: 10.1016/S0140-6736(13)60024-0.
- [9] A. V. Berglar, S. S. Vembar, Past, present and future of malaria prevalence and eradication in the light of climate change, *Elsevier Inc., 2nd ed.*, 2019, doi: 10.1016/B978-0-12-409548-9.11416-2.
- [10] S. Reeha, M. T. Nikhil, A. Thakur, A deep learning approach for prediction of binding affinity for anti malarial drugs and their target proteins, *3rd International Conference on Innovative Technology*, INOCONI, 2024, 1–5, doi: 10.1109/INOCON60754.2024.10512173.
- [11] L. H. Miller, H. C. Ackerman, X. Su, T. E. Wellems, Malaria biology and disease pathogenesis: insights for new treatments, *Nature Medicine*, 2013, **19**, 156–167, doi: 10.1038/nm.3073.
- [12] N. J. White, S. Pukrittayakamee, T. T. Hien, M. A. Faiz, O. A. Mokuolu, A. M. Dondorp, *Malaria, The Lancet*, 2014, **383**, 723–735, doi: 10.1016/S0140-6736(13)60024-0.
- [13] W. J. Moss, S. N. Shah, R. H. Morrow, The history of malaria and its control, *International Encyclopedia of Public Health*, 2008, 389–398.
- [14] L. Platon, D. Ménard, *Plasmodium falciparum* ring-stage plasticity and drug resistance, *Trends in Parasitology*, 2024, **40**, 118–130, doi: 10.1016/j.pt.2023.11.007.
- [15] CDC - DPDx - *Malaria*, <https://www.cdc.gov/dpdx/malaria/index.html>, (accessed November 27, 2024).

- [16] K. Venkatesan, S. B. Rahayu, M. Muthulakshmi and V. P. Velkur, Implementation of Convolutional Neural Network Malarial Cells Detection, *International Conference on Communication, Computing and Internet of Things (IC3IoT)*, Chennai, India, 2024, 1-6, doi: 10.1109/IC3IoT60841.2024.10550234.
- [17] S. Anil Kumar, Amrita Thakur, Sreeharsha Nagaraja; Computational studies on chloroquine derivatives as anti-malarial drugs. *AIP Conf. Proc.*, 13 August 2024, **3196**(1), 060005, <https://doi.org/10.1063/5.0227883>.
- [18] Malaria vaccines (RTS,S and R21), <https://www.who.int/news-room/questions-and-answers/item/q-a-on-rt-s-s-malaria-vaccine>, (accessed May 18, 2024).
- [19] E. Kokori, G. Olatunji, A. Akinboade, A. Akinoso, E. Egbunu, S. A. Aremu, *et al.*, Triple artemisinin-based combination therapy (TACT): advancing malaria control and eradication efforts, *Malaria Journal*, 2024, **23**, 1–7, doi: 10.1186/s12936-024-04844-y.
- [20] M. Sharma, V. Pandey, G. Poli, T. Tuccinardi, M. L. Lolli, V. K. Vyas, A comprehensive review of synthetic strategies and SAR studies for the discovery of PfDHODH inhibitors as antimalarial agents. Part 1: triazolopyrimidine, isoxazolopyrimidine and pyrrole-based (DSM) compounds, *Bioorganic Chemistry*, 2024, **146**, 107249, doi: 10.1016/j.bioorg.2024.107249.
- [21] M. R. Luth, P. Gupta, S. Otilie, E. A. Winzeler, Using in vitro evolution and whole genome analysis to discover next generation targets for antimalarial drug discovery, *ACS Infectious Diseases*, 2018, **4**, 301–314, doi: 10.1021/acsinfecdis.7b00276.
- [22] M. A. Phillips, K. L. White, S. Kokkonda, X. Deng, J. White, F. El Mazouni, *et al.*, A triazolopyrimidine-based dihydroorotate dehydrogenase inhibitor with improved drug-like properties for treatment and prevention of malaria, *ACS Infectious Diseases*, 2016, **2**, 945–957, doi: 10.1021/acsinfecdis.6b00144.
- [23] M. B. Jiménez-Díaz, D. Ebert, Y. Salinas, A. Pradhan, A. M. Lehane, M. E. Myrand-Lapierre, *et al.*, (+)-SJ733, a clinical candidate for malaria that acts through ATP4 to induce rapid host-mediated clearance of Plasmodium, *Proceedings of the National Academy of Sciences*, 2014, **111**, E5455–E5462, doi: 10.1073/pnas.1414221111.
- [24] M. F. Chughlay, E. Rossignol, C. Donini, M. El Gaaloul, U. Lorch, S. Coates, *et al.*, First-in-human clinical trial to assess the safety, tolerability and pharmacokinetics of P218, a novel candidate for malaria chemoprotection, *British Journal of Clinical Pharmacology*, 2020, **86**, 1113–1124.
- [25] A. P. Phyto, P. Jittamala, F. H. Nosten, S. Pukrittayakamee, M. Imwong, N. J. White, *et al.*, Antimalarial activity of artefenomel (OZ439), a novel synthetic antimalarial endoperoxide, in patients with Plasmodium falciparum and Plasmodium vivax malaria: an open-label phase 2 trial, *The Lancet Infectious Diseases*, 2016, **16**, 61–69, doi: 10.1016/S1473-3099(15)00320-5.
- [26] B. Ogutu, A. Yeka, S. Kusemererwa, R. Thompson, H. Tinto, A. O. Toure, *et al.*, Ganaplacide (KAF156) plus lumefantrine solid dispersion formulation combination for uncomplicated Plasmodium falciparum malaria: an open-label, multicentre, parallel-group, randomised, controlled, phase 2 trial, *The Lancet Infectious Diseases*, 2023, **23**, 1051–1061, doi: 10.1016/S1473-3099(23)00209-8.
- [27] T. Yang, S. Otilie, E. S. Istvan, K. P. Godinez-Macias, A. K. Lukens, B. Baragaña, *et al.*, MalDA, accelerating malaria drug discovery, *Trends in Parasitology*, 2021, **37**, 493–507, doi: 10.1016/j.pt.2021.01.009.
- [28] J. E. Hyde, Targeting purine and pyrimidine metabolism in human apicomplexan parasites, *Current Drug Targets*, 2007, **8**, 31–47, doi: 10.2174/138945007779315524.
- [29] M. A. Phillips, P. K. Rathod, Plasmodium dihydroorotate dehydrogenase: a promising target for novel anti-malarial chemotherapy, *Infectious Disorders - Drug Targets*, 2010, **10**, 226–239, doi: 10.2174/187152610791163336.
- [30] X. Deng, D. Matthews, P. K. Rathod, M. A. Phillips, The X-ray structure of Plasmodium falciparum dihydroorotate dehydrogenase bound to a potent and selective N-phenylbenzamide inhibitor reveals novel binding-site interactions, *Acta Crystallographica Section F: Structural Biology Communications*, 2015, **71**, 553–559, doi: 10.1107/S2053230X15000989.
- [31] J. White, S. K. Dhingra, X. Deng, F. El Mazouni, M. C. S. Lee, G. A. Afanador, *et al.*, Identification and mechanistic understanding of dihydroorotate dehydrogenase point mutations in Plasmodium falciparum that confer in vitro resistance to the clinical candidate DSM265, *ACS Infectious Diseases*, 2019, **5**, 90–101, doi: 10.1021/acsinfecdis.8b00211.
- [32] A. C. Pippione, S. Sainas, P. Goyal, I. Fritzson, G. C. Cassiano, A. Giraud, *et al.*, Hydroxyazole scaffold-based Plasmodium falciparum dihydroorotate dehydrogenase inhibitors: synthesis, biological evaluation and X-ray structural studies, *European Journal of Medicinal Chemistry*, 2019, **163**, 266–280, doi: 10.1016/j.ejmech.2018.11.044.
- [33] S. Kokkonda, X. Deng, K. L. White, F. El Mazouni, J. White, D. M. Shackleford, *et al.*, Lead optimization of a pyrrole-based dihydroorotate dehydrogenase inhibitor series for the treatment of malaria, *Journal of Medicinal Chemistry*, 2020, **63**, 4929–4956, doi: 10.1021/acsjmedchem.0c00311.
- [34] S. Kokkonda, F. El Mazouni, K. L. White, J. White, D. M. Shackleford, M. J. Lafuente-Monasterio, *et al.*, Isoxazolopyrimidine-based inhibitors of Plasmodium falciparum dihydroorotate dehydrogenase with antimalarial activity, *ACS Omega*, 2018, **3**, 9227–9240, doi: 10.1021/acsomega.8b01573.
- [35] M. J. Palmer, X. Deng, S. Watts, G. Krilov, A. Gerasyuto, S. Kokkonda, *et al.*, Potent antimalarials with development potential identified by structure-guided computational optimization of a pyrrole-based dihydroorotate dehydrogenase inhibitor series, *Journal of Medicinal Chemistry*, 2021, **64**, 6085–6136, doi: 10.1021/acsjmedchem.1c00173.
- [36] RCSB PDB - 7WYF: Plasmodium falciparum dihydroorotate dehydrogenase (DHODH) in complex with its inhibitor 50, <https://www.rcsb.org/structure/7WYF>, (accessed May 23, 2024).
- [37] V. K. Vyas, T. Shukla, K. Tulsian, M. Sharma, S. Patel, Integrated structure-guided computational design of novel substituted quinolizin-4-ones as Plasmodium falciparum

- dihydroorotate dehydrogenase (*Pf*DHODH) inhibitors, *Computational Biology and Chemistry*, 2022, **101**, 107787, doi: 10.1016/j.compbiolchem.2022.107787.
- [38] A. A. Alzain, Z. A. M. Ahmed, M. A. Mahadi, E. A. Khairy, F. A. Elbadwi, Identification of novel Plasmodium falciparum dihydroorotate dehydrogenase inhibitors for malaria using in silico studies, *Scientific African*, 2022, **16**, e01214, doi: 10.1016/j.sciaf.2022.e01214.
- [39] A. Manhas, M. Y. Lone, P. C. Jha, Multicomplex-based pharmacophore modeling coupled with molecular dynamics simulations: an efficient strategy for the identification of novel inhibitors of *Pf*DHODH, *Journal of Molecular Graphics and Modelling*, 2017, **75**, 413–423, doi: 10.1016/j.jmkgm.2017.04.025.
- [40] E. M. Elamin, S. E. Eshage, S. M. Mohmmode, R. M. Mukhtar, M. Mahjoub, E. Sadelin, *et al.*, Discovery of dual-target natural antimalarial agents against DHODH and PMT of Plasmodium falciparum: pharmacophore modelling, molecular docking, quantum mechanics, and molecular dynamics simulations, SAR and QSAR in *Environmental Research*, 2023, **34**, 709–728, doi: 10.1080/1062936X.2023.2251876.
- [41] Z. Y. Ibrahim, A. Uzairu, G. Shallangwa, S. Abechi, QSAR and molecular docking based design of some indolyl-3-ethanone- α -thioethers derivatives as Plasmodium falciparum dihydroorotate dehydrogenase (*Pf*DHODH) inhibitors, *SN Applied Sciences*, 2020, **2**, 1004, doi: 10.1007/s42452-020-2955-1.
- [42] Z. Y. Ibrahim, A. Uzairu, G. A. Shallangwa, S. E. Abechi, Application of QSAR method in the design of enhanced antimalarial derivatives of azetidine-2-carbonitriles, their molecular docking, drug-likeness, and SwissADME properties, *Iranian Journal of Pharmaceutical Research*, 2021, **20**, 254–270, doi: 10.22037/ijpr.2021.114536.14901.
- [43] M. Maetani, N. Kato, V. A. P. Jabor, F. A. Calil, M. C. Nonato, C. A. Scherer, *et al.*, Discovery of antimalarial azetidine-2-carbonitriles that inhibit P. falciparum dihydroorotate dehydrogenase, *ACS Medicinal Chemistry Letters*, 2017, **8**, 438–442, doi: 10.1021/acsmedchemlett.7b00030.
- [44] B. Salehi, C. Quispe, I. Chamkhi, N. El Omari, A. Balahbib, J. Sharifi-Rad, *et al.*, Pharmacological properties of chalcones: a review of preclinical including molecular mechanisms and clinical evidence, *Frontiers in Pharmacology*, 2021, **11**, 592654, doi: 10.3389/fphar.2020.592654.
- [45] M. Thillainayagam, K. Malathi, S. Ramaiah, In-silico molecular docking and simulation studies on novel chalcone and flavone hybrid derivatives with 1, 2, 3-triazole linkage as vital inhibitors of Plasmodium falciparum dihydroorotate dehydrogenase, *Journal of Biomolecular Structure and Dynamics*, 2018, **36**, 3993–4009, doi: 10.1080/07391102.2017.1404935.
- [46] M. J. Palmer, X. Deng, S. Watts, G. Krilov, A. Gerasuto, S. Kokkonda, *et al.*, Potent antimalarials with development potential identified by structure-guided computational optimization of a pyrrole-based dihydroorotate dehydrogenase inhibitor series, *Journal of Medicinal Chemistry*, 2021, **64**, 6085–6136, doi: 10.1021/acs.jmedchem.1c00173.
- [47] P. A. Akinnusi, S. O. Olubode, A. O. Adebesein, T. J. Osadipe, D. O. Nwankwo, A. D. Adebisi, *et al.*, Structure-based scoring of anthocyanins and molecular modeling of *Pf*LDH, *Pf*DHODH, and *Pf*DHFR reveal novel potential P. falciparum inhibitors, *Informatics in Medicine Unlocked*, 2023, **38**, 101206, doi: 10.1016/j.imu.2023.101206.
- [48] Z. Y. Ibrahim, A. Uzairu, G. A. Shallangwa, S. E. Abechi, S. Isyaku, Computer-aided molecular design of 2-anilino 4-amino substituted quinazolines derivatives as malarial inhibitors, *SN Applied Sciences*, 2021, **3**, 500, doi: 10.1007/s42452-021-04748-5.
- [49] A. H. Haredi Abdelmonsef, M. Eldeeb Mohamed, M. El-Naggar, H. Temairk, A. Mohamed Mosallam, Novel quinazolin-2,4-dione hybrid molecules as possible inhibitors against malaria: synthesis and in silico molecular docking studies, *Frontiers in Molecular Biosciences*, 2020, **7**, 105, doi: 10.3389/fmolb.2020.00105.
- [50] A. Amanatie, J. Jumina, M. Mustofa, M. Hanafi, L. O. Kadidae, I. Sahidin, Synthesis of 2-hydroxyxanthone from xanthone as a basic material for new antimalarial drugs, *Asian Journal of Pharmaceutical and Clinical Research*, 2017, **10**, 242–246, doi: 10.22159/ajpcr.2017.v10i12.19858.
- [51] J. Syahri, E. Yuanita, B. A. Nurohmah, M. H. Wathon, R. Syafri, R. Armunanto, *et al.*, Xanthone as antimalarial: QSAR analysis, synthesis, molecular docking and in-vitro antimalarial evaluation, *Oriental Journal of Chemistry*, 2017, **33**, 29–40, doi: 10.13005/ojc/330104.
- [52] L. P. Hastuti, F. Hermawan, M. R. Iresha, T. Ernawati, Firdayani, In-silico studies of hydroxyxanthone derivatives as potential *Pf*DHFR and *Pf*DHODH inhibitor by molecular docking, molecular dynamics simulation, MM-PBSA calculation and pharmacokinetics prediction, *Informatics in Medicine Unlocked*, 2024, **47**, 101485, doi: 10.1016/j.imu.2024.101485.
- [53] C. Agoni, E. Y. Salifu, G. Munsamy, F. A. Olotu, M. Soliman, CF3-pyridinyl substitution on antimalarial therapeutics: probing differential ligand binding and dynamical inhibitory effects of a novel triazolopyrimidine-based inhibitor on Plasmodium falciparum dihydroorotate dehydrogenase, *Chemistry and Biodiversity*, 2019, **16**, e1900365, doi: 10.1002/cbdv.201900365.
- [54] R. Rawat, S. M. Verma, An exclusive computational insight toward molecular mechanism of MMV007571, a multitarget inhibitor of Plasmodium falciparum, *Journal of Biomolecular Structure and Dynamics*, 2020, **38**, 5362–5373, doi: 10.1080/07391102.2019.1700165.
- [55] B. K. Dickerman, B. Elsworth, S. A. Cobbold, C. Q. Nie, M. J. McConville, B. S. Crabb, *et al.*, Identification of inhibitors that dually target the new permeability pathway and dihydroorotate dehydrogenase in the blood stage of Plasmodium falciparum, *Scientific Reports*, 2016, **6**, 37502, doi: 10.1038/srep37502.
- [56] K. A. Oluwafemi, O. E. Oyenyin, D. D. Babatunde, E. B. Agbaffa, J. A. Aigbogun, O. O. Odeja, *et al.*, Parasitic protozoans: exploring the potential of N,N'-bis[2-(5-bromo-7-azabenzimidazol-1-yl)-2-oxoethyl]ethylene-1,3-diamine and its cyclohexyl-1,2-diamine analogue as TryR and Pf-DHODH inhibitors, *Acta Parasitologica*, 2023, **68**, 807–819, doi: 10.1007/s11686-023-00719-5.

- [57] Z. Y. Ibrahim, A. Uzairu, G. A. Shallangwa, S. E. Abechi, S. Isyaku, Virtual screening and molecular dynamic simulations of the antimalarial derivatives of 2-anilino 4-amino substituted quinazolines docked against a Pf-DHODH protein target, *Egyptian Journal of Medical Human Genetics*, 2022, **23**, 100, doi: 10.1186/s43042-022-00329-2.
- [58] J. Jones, R. D. Clark, M. S. Lawless, D. W. Miller, M. Waldman, The AI-driven drug design (AIDD) platform: an interactive multi-parameter optimization system integrating molecular evolution with physiologically based pharmacokinetic simulations, *Journal of Computer-Aided Molecular Design*, 2024, **38**, **8**, doi: 10.1007/s10822-024-00552-6.
- [59] A. H. Lima Costa, K. S. Bezerra, J. X. de Lima Neto, J. I. N. Oliveira, D. S. Galvão, U. L. Fulco, Deciphering interactions between potential inhibitors and the Plasmodium falciparum DHODH enzyme: a computational perspective, *The Journal of Physical Chemistry B*, 2023, **127**, 9461–9475, doi: 10.1021/acs.jpcc.3c05738.
- [60] Z. Nie, R. Bonnert, J. Tsien, X. Deng, C. Higgs, F. El Mazouni, X. Zhang, R. Li, N. Ho, V. Feher, J. Paulsen, D. M. Shackelford, K. Katneni, G. Chen, A. C. F. Ng, M. McInerney, W. Wang, J. Saunders, D. Collins, D. Yan, P. Li, M. Campbell, R. Patil, A. Ghoshal, P. Mondal, A. Kundu, R. Chittimalla, M. Mahadeva, S. Kokkonda, J. White, R. Das, P. Mukherjee, I. Angulo-Barturen, M. B. Jiménez-Díaz, R. Malmstrom, M. Lawrenz, A. Rodriguez-Granillo, P. K. Rathod, D. R. Tomchick, M. J. Palmer, B. Laleu, T. Qin, S. A. Charman, M. A. Phillips, Structure-based discovery and development of highly potent dihydroorotate dehydrogenase inhibitors for malaria chemoprevention, *Journal of Medicinal Chemistry*, 2025, **68**, 590-637, doi: 10.1021/acs.jmedchem.4c02394.
- [61] P. J. P. Tjitda, F. O. Nitbani, T. D. Wahyuningsih, R. I. Lerrick, Y. M. Abanit, In silico study revealing the inhibitory potential of flavonoids from azadirachta indica against PfDHFR and PfDHODH as antimalarial agents, *ChemistrySelect*, 2025, **10**, doi: 10.1002/slct.202404851.
- [62] S. Lopez-Mercado, C. Enríquez, J. A. Valderrama, R. Pino-Rios, L. Ruiz-Vásquez, L. Ruiz Mesia, G. Vargas-Arana, P. Buc Calderon, J. Benites, Exploring the antibacterial and antiparasitic activity of phenylamino naphthoquinones-green synthesis, biological evaluation and computational study, *International Journal of Molecular Sciences*, 2024, **25**, 10670, doi: 10.3390/ijms251910670
- [63] M. Rani, J. Devi, B. Kumar, M. Rathi, unveiling anti-malarial, antimicrobial, antioxidant efficiency and molecular docking study of synthesized transition metal complexes derived from heterocyclic Schiff base ligands, *Chemistry An Asian Journal*, 2024, **19**, e202400676, doi: 10.1002/asia.202400676.
- [64] D. O. Adekunle, E. O. Faboro, L. Lajide, Molecular docking and pharmacokinetics studies of selected anthraquinone compounds with possible anti-plasmodial properties of Morinda lucida, *Letters in Applied NanoBioScience*, 2024, **13**, 91, doi: 10.33263/LIANBS132.09.
- neutral with regard to jurisdictional claims in published maps and institutional affiliations.

Open Access

This article is licensed under a Creative Commons Attribution 4.0 International License, which permits use, sharing, adaptation, distribution and reproduction in any medium or format, as long as you give appropriate credit to the original author(s) and the source, provide a link to the Creative Commons licence, and indicate if changes were made. The images or other third-party material in this article are included in the article's Creative Commons licence, unless indicated otherwise in a credit line to the material. If material is not included in the article's Creative Commons licence and your intended use is not permitted by statutory regulation or exceeds the permitted use, you will need to obtain permission directly from the copyright holder. To view a copy of this licence, visit <http://creativecommons.org/licenses/by/4.0/>.

© The Author(s) 2025.